

# nature climate change

JUNE 2013 VOL 3 NO 6  
[www.nature.com/natureclimatechange](http://www.nature.com/natureclimatechange)

## Mussels lose their grip

### ATMOSPHERIC CIRCULATION

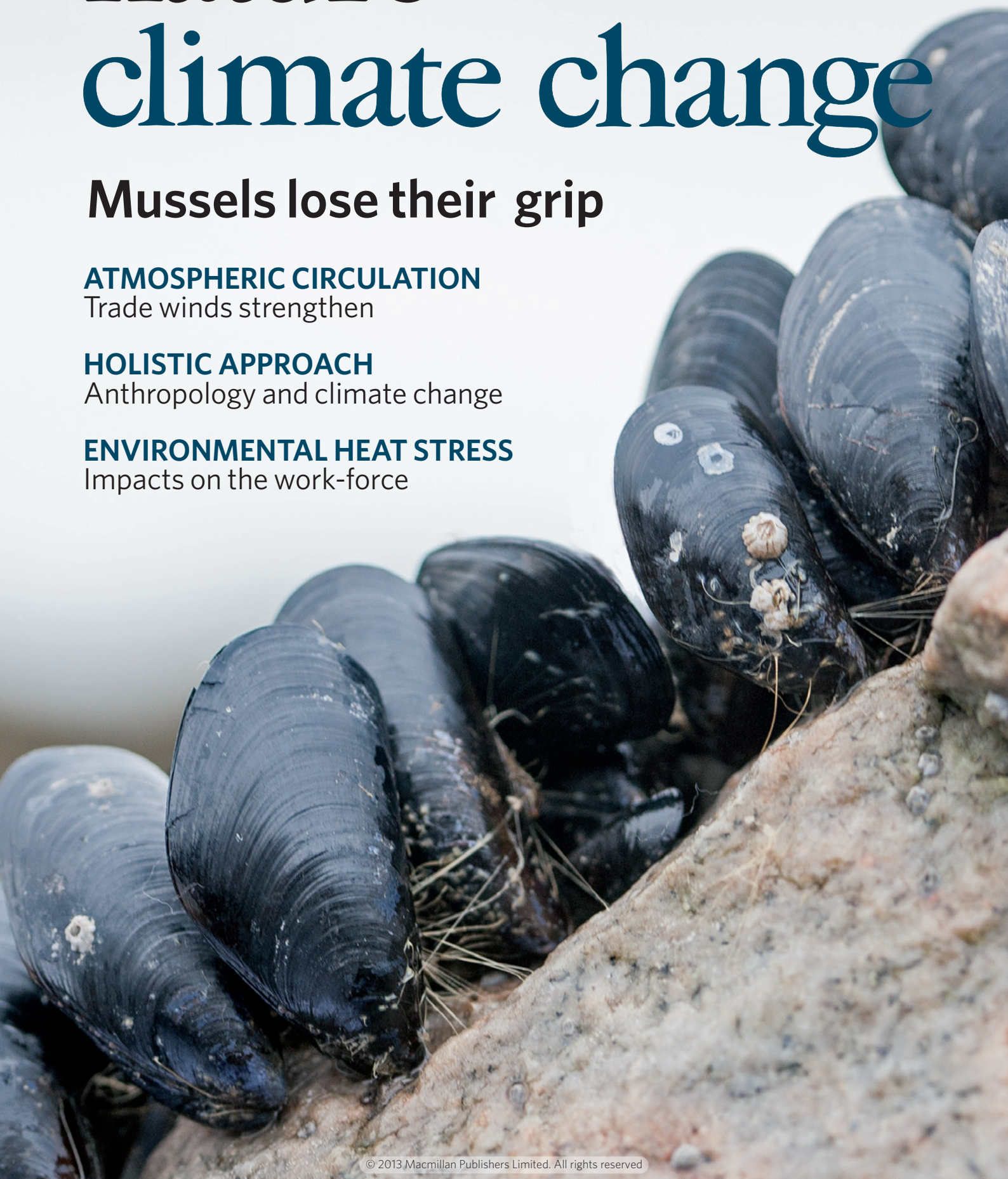
Trade winds strengthen

### HOLISTIC APPROACH

Anthropology and climate change

### ENVIRONMENTAL HEAT STRESS

Impacts on the work-force



# Mussel byssus attachment weakened by ocean acidification

Michael J. O'Donnell<sup>1\*</sup>, Matthew N. George<sup>1,2</sup> and Emily Carrington<sup>1,2</sup>

**Biomaterials connect organisms to their environments. Their function depends on biological, chemical and environmental factors, both at the time of creation and throughout the life of the material. Shifts in the chemistry of the oceans driven by anthropogenic CO<sub>2</sub> (termed ocean acidification) have profound implications for the function of critical materials formed under these altered conditions. Most ocean acidification studies have focused on one biomaterial (secreted calcium carbonate), frequently using a single assay (net rate of calcification) to quantify whether reductions in environmental pH alter how organisms create biomaterials<sup>1</sup>. Here, we examine biological structures critical for the success of ecologically and economically important bivalve molluscs. One non-calcified material, the proteinaceous byssal threads that anchor mytilid mussels to hard substrates, exhibited reduced mechanical performance when secreted under elevated pCO<sub>2</sub> conditions, whereas shell and tissue growth were unaffected. Threads made under high pCO<sub>2</sub> (>1,200 µatm) were weaker and less extensible owing to compromised attachment to the substratum. According to a mathematical model, this reduced byssal fibre performance, decreasing individual tenacity by 40%. In the face of ocean acidification, weakened attachment presents a potential challenge for suspension-culture mussel farms and for intertidal communities anchored by mussel beds.**

Coastal regions host rich and diverse communities of organisms and are the primary location of contact between human activities and the oceans. Understanding the biological consequences of environmental changes in these areas is critical to predicting what ecosystems will look like in the future. As human activities release CO<sub>2</sub> to the atmosphere, and that CO<sub>2</sub> dissolves into the surface ocean, seawater pH declines, a process known as ocean acidification<sup>2</sup>. This presents a new set of challenges to organisms living on rocky shores. Open-ocean systems are predicted to experience declines of ~0.2 pH units over the twenty-first century. Nearshore systems already experience lower and more variable pH water owing to coastal upwelling and high levels of biological activity<sup>3</sup>. Over the past 20 years, worldwide research efforts have discovered a wide variety of organisms and biological processes that seem susceptible to reduced pH conditions. Corals, the earliest and perhaps best studied group, exhibit lower growth of calcified structures<sup>4</sup>. Echinoderms, particularly at vulnerable larval stages, experience lower growth and altered stress responses<sup>5</sup>. The relatively few studies on mussels have shown slower growth<sup>6</sup>, reduced immune response<sup>7</sup> and slower larval growth with weaker shells<sup>8</sup>.

Mytilid mussels are both ecologically and economically important. They are competitive dominants for space on rocky shores worldwide, largely owing to their ability to adhere to bare rock

with byssal threads. Mussels also support a worldwide aquaculture industry worth more than US\$1.5 billion in 2009<sup>9</sup>. The byssal threads of mytilid mussels are formed from collagen-like liquid precursors that are secreted into a groove in the foot and polymerize into a stiff yet extensible thread<sup>10,11</sup>. Byssal threads are divided into three distinct regions: a highly extensible proximal end, a distal portion that is initially stiff, but yields (plastically deforms) before stiffening again, and a plaque that adheres the thread to the substratum<sup>12</sup>. Previous studies have shown that threads typically fail at the plaque or proximal regions<sup>10,12</sup>. The chemical properties of byssal threads have been well documented as well<sup>11,13,14</sup>. Byssal threads include a high concentration of the modified amino acid 3,4-dihydroxyphenylalanine (Dopa) and histidine–metal crosslinkages, which seem to play critical roles in surface adhesion and self-healing following deformation<sup>11,15</sup>. These chemical functions are known to depend on pH, including shifts in the His–metal crosslinks responsible for some of the thread stiffness properties<sup>11</sup>, motivating interest in how this biomaterial might be affected by shifts in ocean chemistry. Importantly, external seawater chemistry may mediate byssal thread formation in a manner that is not detectable using genomic, transcriptomic or proteomic techniques; we report here effects of elevated CO<sub>2</sub> on the end phenotype.

In addition to their primary chemistry, byssal strength is known to be affected by other aspects of the environment and mussel physiology, including seasonal effects and tradeoffs with reproductive condition<sup>16</sup>. We looked at several aspects of mussel physiology including growth, general condition and reproductive status to explore possible linkages between condition and byssus strength. Making ecomechanical predictions (*sensu* refs 17,18) about future communities requires examining the response function of a variety of biological parameters to a wide range of pCO<sub>2</sub> scenarios.

As the pCO<sub>2</sub> in the water increased from 300 to 1,500 µatm (pH decline from 8.0 to 7.5 on the total scale, within the range observed in mussel beds<sup>19</sup>), individual threads broke at lower forces and extensions (Fig. 1a). This result was driven entirely by plaque weakening (Fig. 2a); mechanical performance was unchanged in the proximal (Fig. 2b) and distal regions (not shown). Consequently, the most probable location of failure moved from the proximal region to the plaque in more acidic treatments (Fig. 2c). Although there was no effect of pCO<sub>2</sub> treatment on the force at which the distal region yielded (Fig. 2a), overall thread extensibility decreased at the higher pCO<sub>2</sub> treatments (Fig. 1b) because the plaque frequently failed before the distal region fully yielded (Figs 1c and 2a).

As extensible byssal threads spread hydrodynamic loads evenly across many threads of the byssus<sup>12</sup>, reduced thread strength and extensibility combine to limit the tenacity, or ability of

<sup>1</sup>Friday Harbor Laboratories, University of Washington, 620 University Road, Friday Harbor, Washington 98250, USA, <sup>2</sup>Department of Biology, University of Washington, Seattle, Washington 98195, USA. \*e-mail: mooseo@uw.edu.

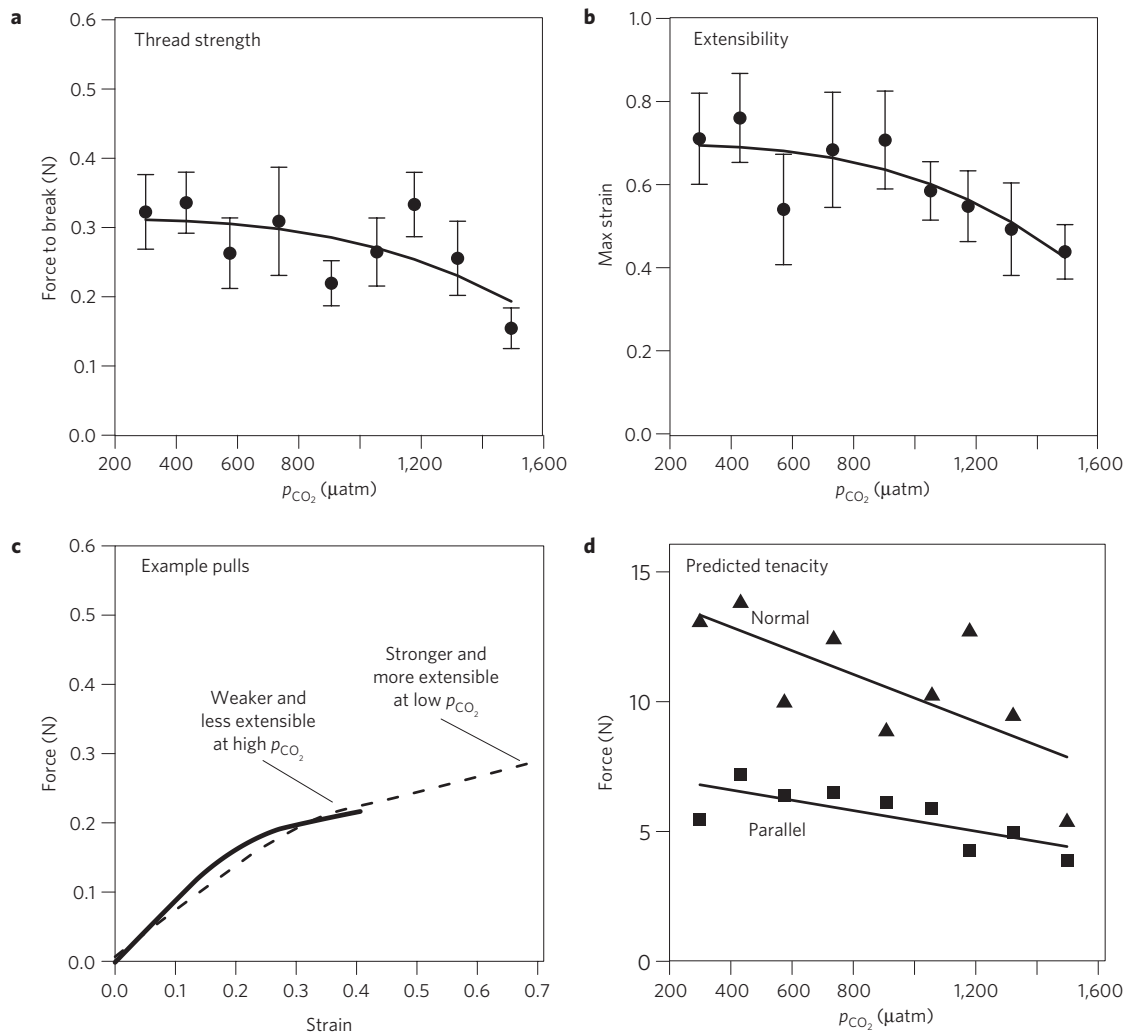


**Figure 1 | Performance of byssal threads as a function of  $p_{CO_2}$  treatment.** **a,b**, Whole threads are significantly weaker (mean,  $n = 8 \pm \text{s.e.m.}$ , breaking force =  $0.31 - 3.55 \times 10^{-11} * (p_{CO_2})^3$ ,  $p < 0.05$ ; **a**), and are significantly less extensible with increased  $p_{CO_2}$  (mean,  $n = 8 \pm \text{s.e.m.}$ , breaking strain =  $0.07 - 8.11 \times 10^{-11} * (p_{CO_2})^3$ ,  $p < 0.01$ ; **b**). **c**, Representative tensile tests of whole threads showing distal region yield and subsequent failure when  $p_{CO_2} < 1,200 \mu\text{atm}$  (dashed line). At high  $p_{CO_2}$ , threads more often fail in the plaque region before the distal region fully yields (solid line). **d**, Predicted model of whole-animal tenacity when pulled normal (triangles) or parallel (squares) to substratum. In both cases, there is a significant decline in tenacity as a function of  $p_{CO_2}$  ( $p < 0.05$ ; normal: 41% decline, parallel: 35% decline).

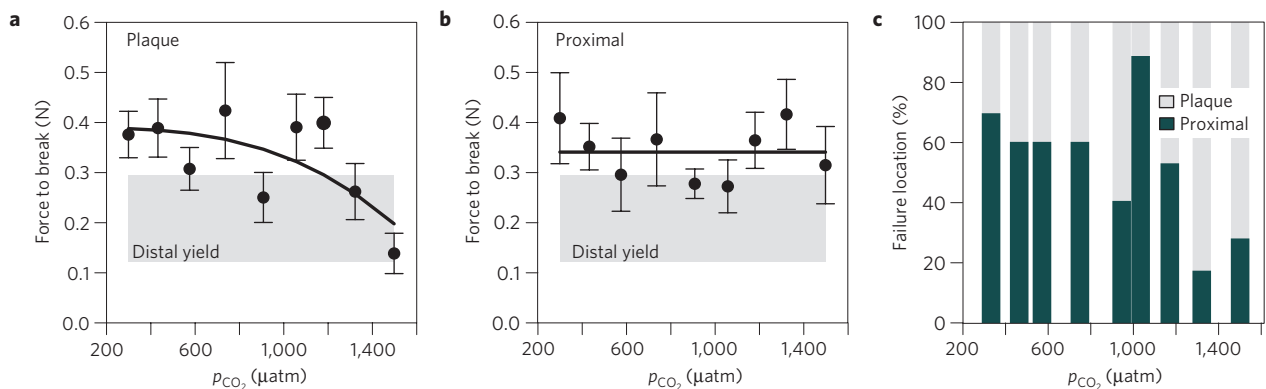


**Figure 2 | Performance of byssal thread components.** **a,b**, Plaques weaken with increased  $p_{CO_2}$  (mean,  $n = 8 \pm \text{s.e.m.}$  force =  $0.39 - 5.70 \times 10^{-11} * (p_{CO_2})^3$ ,  $p < 0.05$ ; **a**), whereas the structural integrity of the proximal region is maintained (symbols are mean  $\pm$  s.e.m.,  $n = 8$ , line is pooled mean,  $p = 0.73$ ; **b**). Distal yield force (represented by shaded region of mean  $\pm$  s.d.) was also unaffected by  $p_{CO_2}$  ( $p = 0.90$ ). **c**, At lower  $p_{CO_2}$ , failure commonly occurs in either the proximal region (dark shading) or plaque (light shading). At high  $p_{CO_2}$  ( $> 1,200 \mu\text{atm}$ ) there is a higher likelihood of plaque failure.

**Table 1 | Water conditions during 20-day experiment.**

$p_{\text{CO}_2}$ target ( $\mu\text{atm}$ )	Temp ( $^{\circ}\text{C}$ )	pH (total scale)	Totally alkalinity ( $\mu\text{mol kg}^{-1}$ )	Total carbon ( $\mu\text{mol kg}^{-1}$ )	$p_{\text{CO}_2}$ ( $\mu\text{atm}$ )	$\Omega_{\text{Ar}}$	$\Omega_{\text{Ca}}$
300	10.8 $\pm$ 0.6	8.14 $\pm$ 0.02	2,081	1,896 $\pm$ 23	299 $\pm$ 8	2.0	3.2
500	10.6 $\pm$ 0.6	8.00 $\pm$ 0.02	2,086	1,955 $\pm$ 12	432 $\pm$ 15	1.5	2.4
600	10.2 $\pm$ 0.8	7.89 $\pm$ 0.04	2,084	1,993 $\pm$ 11	575 $\pm$ 16	1.2	1.9
800	10.2 $\pm$ 0.6	7.79 $\pm$ 0.05	2,083	2,020 $\pm$ 20	736 $\pm$ 37	1.0	1.5
1,000	10.4 $\pm$ 0.7	7.70 $\pm$ 0.06	2,085	2,045 $\pm$ 19	908 $\pm$ 89	0.8	1.3
1,100	10.5 $\pm$ 0.5	7.64 $\pm$ 0.04	2,082	2,058 $\pm$ 16	1,057 $\pm$ 95	0.7	1.1
1,200	10.1 $\pm$ 0.6	7.60 $\pm$ 0.02	2,088	2,077 $\pm$ 14	1,180 $\pm$ 119	0.6	1.0
1,300	10.4 $\pm$ 0.6	7.55 $\pm$ 0.04	2,086	2,088 $\pm$ 17	1,322 $\pm$ 45	0.6	0.9
1,500	10.4 $\pm$ 0.7	7.50 $\pm$ 0.01	2,087	2,102 $\pm$ 13	1,498 $\pm$ 37	0.5	0.8

Temperature is average  $\pm$  s.d. of daily measures. pH is average of 1-min readings from Durafet electrodes. pH deviation provides an estimate of the accuracy of the measurement technique, and represents the average deviation between recorded pH and pH calculated from six TA and  $T_{\text{C}}$  measurements pairs. TA was estimated from daily salinity as described in text.  $T_{\text{C}}$ ,  $p_{\text{CO}_2}$ ,  $\Omega_{\text{Ar}}$  and  $\Omega_{\text{Ca}}$  (the saturation states of aragonite and calcite, respectively) are averages  $\pm$  s.d. estimated daily from TA and recorded pH using CO2calc.  $p_{\text{CO}_2}$  deviation provides a summary estimate of chemical variability throughout the experiment; it includes the short-term fluctuations in pH and longer-term changes in alkalinity. Water was undersaturated with respect to aragonite in five of the treatments, and with respect to calcite in the highest two treatments.

a mussel to remain on the shore, under wave-induced stress. We employed the model from ref. 12 to estimate the effect of increased  $p_{\text{CO}_2}$  on mussel tenacity. We considered the simple case of a mussel with 50 threads, each with average length, strength and extensibility for a given treatment group. When the model mussel was pulled parallel or normal to the substratum, tenacity decreased 35–41% over the range of  $p_{\text{CO}_2}$  levels tested (Fig. 1d). This ecomechanical analysis suggests that ocean acidification, by changing the properties of byssal thread structures, will reduce mussel tenacity and increase dislodgement risk in natural habitats and commercial suspension cultures<sup>20,21</sup>.

None of the other physiological metrics examined varied across the range of  $p_{\text{CO}_2}$  levels tested. All animals exhibited positive growth during the 20-day experimental period and there was no trend with  $p_{\text{CO}_2}$  treatment (Supplementary Table S1). Given the short-term nature of this exposure, this is not surprising. The lack of pattern in body metrics suggests that the effect we document in byssal thread strength is not a result of reduced physiological condition.

Our knowledge of byssal thread chemistry<sup>11,13</sup>, especially the pH dependence of Dopa, suggests direct linkages between seawater chemistry and thread adhesion. Biochemical studies on these composite materials typically explore pH ranges outside the environmental range (for example, 5.5; ref. 11); our results suggest the importance of further study on these reactions at finer pH resolution. As noted above, under the scenario that pH exerts a direct, chemical effect on byssal thread components, the strong effect of acidification on mussel attachment would be undetectable using transcriptomic or proteomic methods being employed in many ocean acidification studies. Alternatively, it is possible that acidification drives thread weakening by altering some aspect of mussel physiology, although this was not apparent from our measures of reproduction and condition. Still another, non-exclusive, hypothesis is that exposure to increased  $\text{CO}_2$  alters biofilm properties that, in turn, affect plaque attachment<sup>22</sup>. This study was not designed to probe these causal relationships, but in light of the thread weakening presented here, they demand further study.

Ocean acidification will affect marine communities in a variety of ways, and many effects will be mediated by changes in biological materials. Although calcium carbonate materials have received the most attention so far, our results demonstrate that other critical biological structures are susceptible to reduced performance under ocean acidification. Scaling results such as these to the community level requires understanding pivotal interactions between organisms and their environment. In the case of mussels, secure attachment is key to their ecological importance, and decades

of research<sup>16,20,23</sup> provide a robust framework to appreciate the importance of shifts in byssus strength to community dynamics.

## Methods

*Mytilus trossulus* (40–50 mm shell length) were collected from Argyle Creek, San Juan Island, Washington (48° 31' 19.95" N, 123° 0' 51.80" W) and held for two weeks in unfiltered flowing sea water at the Friday Harbor Laboratories. Animals were transferred to flow-through experimental chambers supplied with sea water at controlled pH. Eight replicate experimental chambers were nested at each of 9 pH levels. Control of pH occurred in 150 L insulated mixing reservoirs filled with filtered sea water at 10 °C. A Honeywell UDA2182 pH controller and Honeywell Durafet III electrode monitored the pH of each reservoir and added  $\text{CO}_2$  to maintain the pH at a predefined setpoint calculated from target  $p_{\text{CO}_2}$  levels (Table 1) using CO2calc<sup>24</sup>. The process pH and temperature were measured continuously from the same Durafet electrode used for control. Temperature and salinity were measured daily using a Fluke 1523 thermometer and a Hach Sension 5 conductivity meter. Detailed chemistry, including total alkalinity (TA, SOP 3b from ref. 25) and total dissolved inorganic carbon ( $T_{\text{C}}$ , by acidification and quantification using a Licor LI-700  $\text{CO}_2$  detector), was measured every 3–4 days. We used the relationship between TA and salinity (measured on five occasions: salinity range: 28.9–31.0, TA range: 2033–2130,  $R^2 = 0.95$ ) to estimate daily TA in each chamber. From estimated TA and measured pH, we estimated the  $p_{\text{CO}_2}$  of each chamber on a daily basis (Table 1). To check the accuracy of the Durafet pH probes, we compared the probe value with the pH calculated from TA and  $T_{\text{C}}$  (Table 1).

Two individual mussels were held in each 3.5 L chamber; one mussel was used for byssal thread, shell size, body mass and shell organic content analyses; the other individual was used for shell crushing. Chambers were flow-through, filled from the mixing reservoirs at 50 ml  $\text{min}^{-1}$ , and held within mixing reservoirs to maintain constant temperature. Mussels were fed commercial Shellfish Diet 1800 (Reed Mariculture) at a rate of 5% dry tissue weight  $\text{day}^{-1}$ . Mussels were first held for two weeks to acclimate to experimental conditions; the byssus was then removed from each individual, and allowed to regrow for 20 days. Treatment chambers were lined with  $\sim$ 12 mm pebbles, providing an easily manipulated attachment point for byssal threads. For testing, an individual thread was excised from the byssus, with care taken to avoid loading the thread. The pebble to which the plaque was attached was epoxied to an aluminium bracket and the root of the thread was secured between cardboard with cyanoacrylate. The cardboard and aluminium bracket were secured in the clamps of an Instron 5565 materials testing frame. Byssal threads were tested while submerged in a 10 °C seawater bath by pulling normal to the substratum at 10 mm  $\text{min}^{-1}$  until failure following ref. 26. Thread strength, extensibility and failure location were recorded and unbroken thread portions were subsequently retested to measure distal yield and force to break plaque and proximal regions<sup>12,26</sup>. Distal region failures were rare and excluded. The right valve from the second mussel was crushed between flat plates to test for weakening due to exposure to  $\text{CO}_2$  (ref. 12). Condition and reproductive indices were measured following ref. 16. Organic content of shell was determined by weighing before and after ashing at 500 °C.

Regression analysis was used to evaluate the effect of  $p_{\text{CO}_2}$  on thread performance. We explored a variety of threshold fits using TableCurve 2.0; the most parsimonious curve that exhibited the response we observed visually in some response variables (no change at low  $p_{\text{CO}_2}$  levels, followed by a dropoff above a threshold level) was a third-order polynomial function of the form  $y = a + bx^3$ . We compared this function and a simple linear fit using AIC (Akaike's information criterion) and chose the curve with the lowest score. Regression analyses were carried out on the means of ( $n = 8$ ) mussels from each treatment group using R (ref. 27).

The details of the whole-animal tenacity model are found in ref. 12. Briefly, the model assumed a mussel attached with 50 threads evenly arranged around a circle. Model parameters, including thread initial length, stiffness, maximum strain ( $\epsilon_{\max}$ ) at failure, and force of distal yield were the average values measured in each treatment group. Pulled normal to the substratum, the model loaded all threads evenly until failure; pulled parallel, the model displaced the mussel and recruited further threads once the original threads were sufficiently stretched. At each displacement step, the strain in each thread was calculated. Individual threads failed when  $\epsilon_{\max}$  was reached; the animal was considered dislodged when all threads were broken.

Received 3 November 2012; accepted 4 February 2013;  
published online 10 March 2013

## References

- Kroeker, K. J., Kordas, R. L., Crim, R. N. & Singh, G. G. Meta-analysis reveals negative yet variable effects of ocean acidification on marine organisms. *Ecol. Lett.* **13**, 1419–1434 (2010).
- Ocean Acidification Due to Increasing Atmospheric Carbon Dioxide* Policy document 12/05 (The Royal Society, 2005).
- Feely, R. A., Sabine, C. L., Hernandez-Ayon, J. M., Ianson, D. & Hales, B. Evidence for upwelling of corrosive 'acidified' water onto the continental shelf. *Science* **320**, 1490–1492 (2008).
- Hoegh-Guldberg, O. *et al.* Coral reefs under rapid climate change and ocean acidification. *Science* **318**, 1737–1742 (2007).
- O'Donnell, M. J. *et al.* Ocean acidification alters skeletogenesis and gene expression in larval sea urchins. *Mar. Ecol. Prog. Ser.* **398**, 157–171 (2010).
- Melzner, F. *et al.* Food supply and seawater  $p_{\text{CO}_2}$  impact calcification and internal shell dissolution in the blue mussel *Mytilus edulis*. *PLoS ONE* **6**, e24223 (2011).
- Bibby, R., Widdicombe, S., Parry, H., Spicer, J. & Pipe, R. Effects of ocean acidification on the immune response of the blue mussel *Mytilus edulis*. *Aquat. Biol.* **2**, 67–74 (2008).
- Gaylord, B. *et al.* Functional impacts of ocean acidification in an ecologically critical foundation species. *J. Exp. Biol.* **214**, 2586–2594 (2011).
- FAO Yearbook: Fishery and Aquaculture Statistics, 2009* (Statistics and Information Service of the Fisheries and Aquaculture Department, 2011).
- Carrington, E. & Gosline, J. M. Mechanical design of mussel byssus: Load cycle and strain rate dependence. *Am. Malacol. Bull.* **18**, 135–142 (2004).
- Harrington, M. J. & Waite, J. H. Holdfast heroics: Comparing the molecular and mechanical properties of *Mytilus californianus* byssal threads. *J. Exp. Biol.* **210**, 4307–4318 (2007).
- Bell, E. & Gosline, J. Mechanical design of mussel byssus: Material yield enhances attachment strength. *J. Exp. Biol.* **199**, 1005–1017 (1996).
- Lee, H., Scherer, N. F. & Messersmith, P. B. Single-molecule mechanics of mussel adhesion. *Proc. Natl Acad. Sci. USA* **103**, 12999–13003 (2006).
- Zhao, H. & Waite, J. H. Linking adhesive and structural proteins in the attachment plaque of *Mytilus californianus*. *J. Biol. Chem.* **281**, 26150–26158 (2006).
- Waite, J. H. & Broomell, C. C. Changing environments and structure–property relationships in marine biomaterials. *J. Exp. Biol.* **215**, 873–883 (2012).
- Carrington, E. Seasonal variation in the attachment strength of blue mussels: Causes and consequences. *Limnol. Oceanogr.* **47**, 1723–1733 (2002).
- Denny, M. W. & Gaylord, B. Marine ecomechanics. *Annu. Rev. Mar. Sci.* **2**, 89–114 (2010).
- Denny, M. & Helmuth, B. Confronting the physiological bottleneck: A challenge from ecomechanics. *Integr. Comput. Biol.* **49**, 197–201 (2009).
- Wootton, J. T., Pfister, C. A. & Forester, J. D. Dynamic patterns and ecological impacts of declining ocean pH in a high-resolution multi-year dataset. *Proc. Natl Acad. Sci. USA* **105**, 18848–18853 (2008).
- Carrington, E., Moeser, G. M., Dimond, J., Mello, J. J. & Boller, M. L. Seasonal disturbance to mussel beds: Field test of a mechanistic model predicting wave dislodgment. *Limnol. Oceanogr.* **54**, 978–986 (2009).
- Lachance, A. A., Myrand, B., Tremblay, R., Koutitonsky, V. & Carrington, E. Biotic and abiotic factors influencing attachment strength of blue mussels *Mytilus edulis* in suspended culture. *Aquat. Biol.* **2**, 119–129 (2008).
- Nicklisch, S. C. T. & Waite, J. H. Mini-review: The role of redox in Dopa-mediated marine adhesion. *Biofouling* **28**, 865–877 (2012).
- Paine, R. T. & Levin, S. A. Intertidal landscapes: Disturbance and the dynamics of pattern. *Ecol. Monogr.* **51**, 145–178 (1981).
- Robbins, L. L., Hansen, M. E., Kleypas, J. A. & Meylan, S. C. *CO2calc—A User-friendly Seawater Carbon Calculator for Windows, Mac OS X, and iOS (iPhone)* US Geological Survey Open-File Report 2010-1280 (USGS, 2010).
- Dickson, A. G., Sabine, C. L. & Christian, J. R. (eds) *Guide to Best Practices for Ocean CO<sub>2</sub> Measurements* Vol. 3 (PICES Spec. Publ., 2007).
- Moeser, G. M. & Carrington, E. Seasonal variation in mussel byssal thread mechanics. *J. Exp. Biol.* **209**, 1996–2003 (2006).
- R Development Core Team *R: A Language and Environment for Statistical Computing* (R Foundation for Statistical Computing, 2010).

## Acknowledgements

Thanks to M. Herko and L. Newcomb for assistance with water chemistry and animal care, and L. Miller for help with figures. This work was supported by NSF award #DBI0829486 to K. Sebens, T. Klinger and J. Murray, and by NSF award #EF104113 to E. Carrington.

## Author contributions

M.J.O., E.C. and M.N.G. designed the experiment, analysed data and wrote the paper. M.J.O. and M.N.G. conducted the experiment.

## Additional information

Supplementary information is available in the online version of the paper. Reprints and permissions information is available online at [www.nature.com/reprints](http://www.nature.com/reprints). Correspondence and requests for materials should be addressed to M.J.O.

## Competing financial interests

The authors declare no competing financial interests.